

## STRUCTURE OF NiCrAlY METAL POWDERS

KAROL IŽDINSKÝ, JOZEF IVAN,  
MILINA ZEMÁNKOVÁ, VLADIMÍR KOLENČIAK

Initial structure of metallic powders can be a possible source of structural inhomogeneities found in plasma spray coatings. These powders prepared by rapid solidification techniques result in appropriate non-equilibrium phases and structures. Results of structural studies performed by light microscopy, SEM, TEM, and EDX on NiCrAlY metallic powders are presented in this paper. The structure was found consisting of a mixture of phases including  $\beta$ -NiAl, martensitic NiAl,  $\gamma$  and  $\gamma'$ . Y is bound in Ni<sub>5</sub>Y yttride localized in the grain boundary regions.

## ŠTRUKTÚRA KOVOVÝCH PRÁŠKOV NiCrAlY

Východisková štruktúra práškov môže byť zdrojom štruktúrnych nehomogenít nachádzaných v povlakoch nanášaných plazmou. Tieto prášky sa pripravujú metódami využívajúcimi rýchle tuhnutie, čo vedie ku vzniku príslušných nerovnovážnych fáz a štruktúr. V tomto článku sú uvedené výsledky štúdia štruktúry kovových práškov typu NiCrAlY dosiahnuté pomocou svetelnej mikroskopie, SEM, TEM a EDX. Štruktúra práškov je zložená zo zmesi fáz  $\beta$ -NiAl, martenzitu NiAl,  $\gamma$  a  $\gamma'$ . Yttrium je viazané v ytride Ni<sub>5</sub>Y, ktorý sa nachádza na hraniciach jednotlivých zŕn.

### 1. Introduction

Plasma sprayed coatings naturally possess various kinds of inhomogeneities including pores, voids, unmelted particles, non-equilibrium phases and structures, etc. A serious investigation of sources of these inhomogeneities inevitably requires also a study of the initial structure of powders used in the plasma spraying process. Metallic powders prepared by rapid solidification techniques result in appropriate non-equilibrium structures. It appears that the microstructure of the powders, their phase distribution and chemical segregation of elemental components can considerably effect the structural properties of the coating.

The progress achieved in thin foil preparation techniques makes the study of the structure of powders possible also with TEM. The aim of this paper is to

demonstrate the utilisation of EM preparatory techniques and to present some results achieved by the study of the structure of NiCrAlY (AMDRY 962) metal powders.

## 2. Experimental material and procedure

AMDRY 962 is a nickel base alloy powder with a nominal composition Ni<sub>22</sub>Cr<sub>10</sub>Al<sub>11</sub>O<sub>Y</sub>. The powder is of spherical shape with grain sizes ranging from 106 to 45  $\mu\text{m}$  and is used for protective plasma spray coatings in hot corrosive or oxidizing environments at high temperatures, e.g. to protect gas turbine blades or valve stems and valve chambers in marine diesel engines. It can also be used as a hot corrosion and oxidation resistant interlayer bond coat for thermal barrier zirconia coatings.

Light microscopy (LM), scanning electron microscopy (SEM), transmission electron microscopy (TEM), and energy-dispersive X-ray spectroscopy (EDX) were used for the structural studies. The samples for LM and SEM studies were prepared by embedding the powder in a cold-curing resin with subsequent grinding and polishing in a conventional metallographic way. The thin foil preparation started with a NiCrAlY powder embedding in a melted mixture of four parts of one component glue ARALDIT AT1 and one part of carbon powder. Melting of this mixture begins at about 130°C and the solidification takes place 10 to 15 minutes later. The hardening is finished in 1 hour at 180°C. Mixing carbon into the glue decreases the sputter speed of the bonding material. The sample with the embedded NiCrAlY powder was then mechanically thinned and polished from both sides to the final thickness of  $\sim 50 \mu\text{m}$ . The samples were further thinned down by argon ion bombardment using a 7.5 kV and 1 mA argon ion beam inclined at 10° to the surface. The sample was bombarded for about 20 hours under these conditions. The first hole appeared in the bonding material between the metallic particles. Further thinning proceeded using a 5 kV and 0.5 mA beam until the metallic powders were also perforated.

Electron microscopy observations were carried out at a JEOL JEM 100 C analytical electron microscope equipped with an ultra high resolution scanning system EM-ASID-4D. An accelerating voltage of 20 kV for secondary electron imaging and 100 kV for transmission electron microscopy observations were used. Analyses including bright field and dark field observations with selected area electron diffraction (SAED) were employed. EDX analyses were performed using a Kevex Delta class IV spectrometer with an ultra-thin window detector (Kevex Quantum detector).

## 3. Results

The particles of NiCrAlY powder are mostly of a spherical shape as shown in Fig. 1. Light microscopy observations of the etched cross sectional area revealed

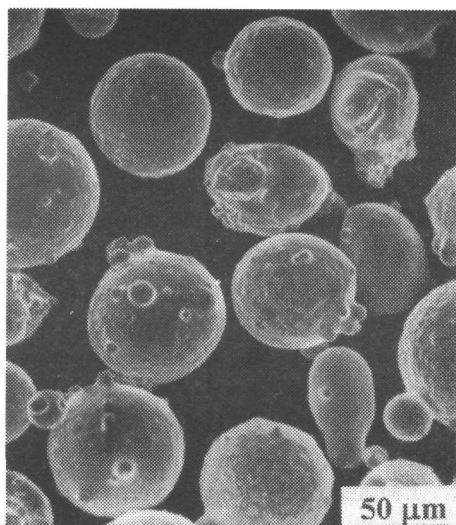


Fig. 1. Secondary electron micrograph of NiCrAlY powder particles.

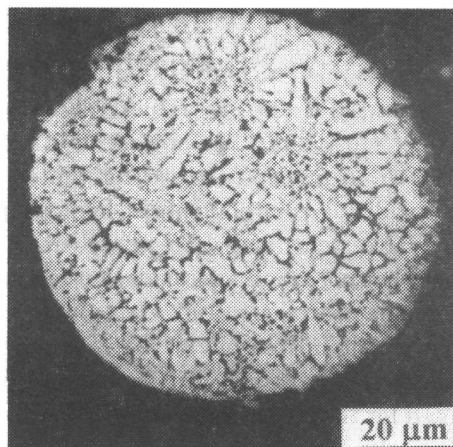


Fig. 2. Light micrograph showing the overall microstructure in a midsection of the NiCrAlY powder.

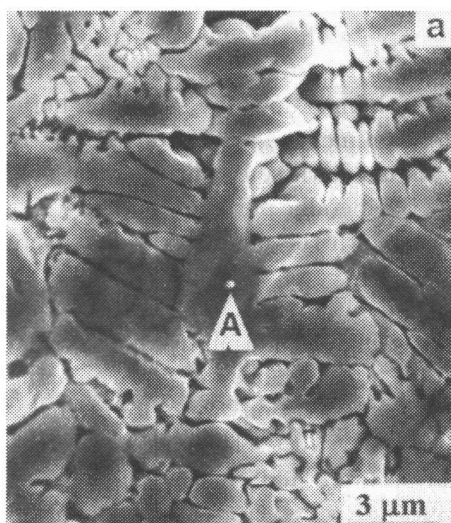


Fig. 3a. Secondary electron micrograph of an Al lean dendrite in the microstructure of the NiCrAlY powder (EDX analysis at A, composition in at.% Ni25Cr7Al).

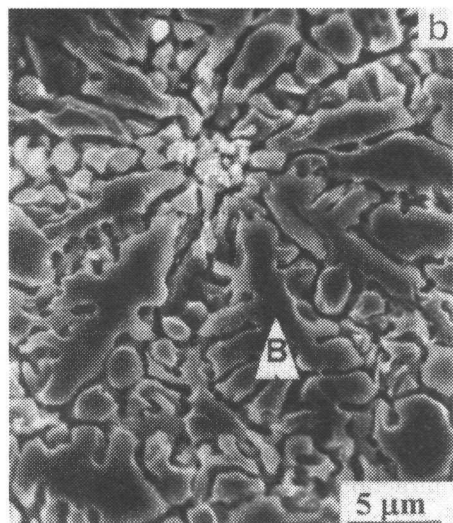


Fig. 3b. Secondary electron micrograph of an Al rich dendrite in the microstructure of the NiCrAlY powder (EDX analysis at B, composition in at.% Ni19Cr30Al).

Fig. 4. Secondary electron micrograph showing a thin foil sample of a NiCrAlY powder particle.

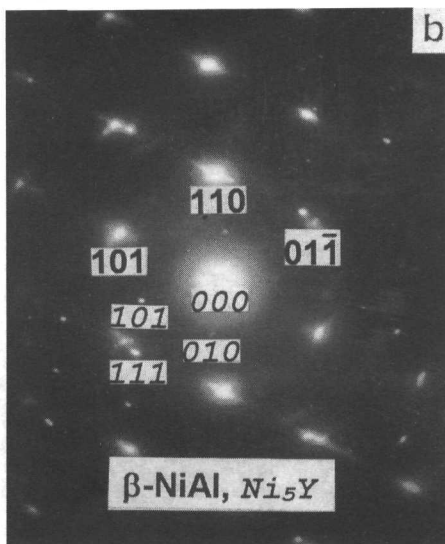
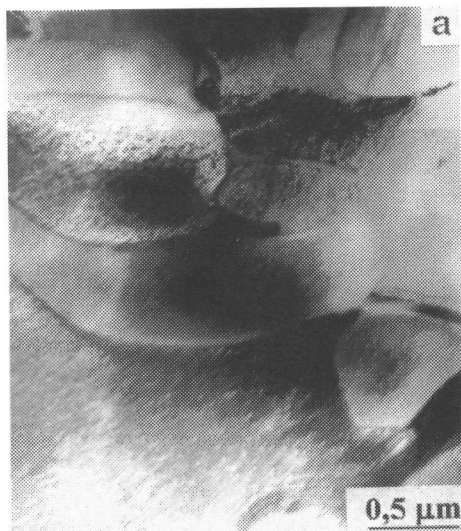
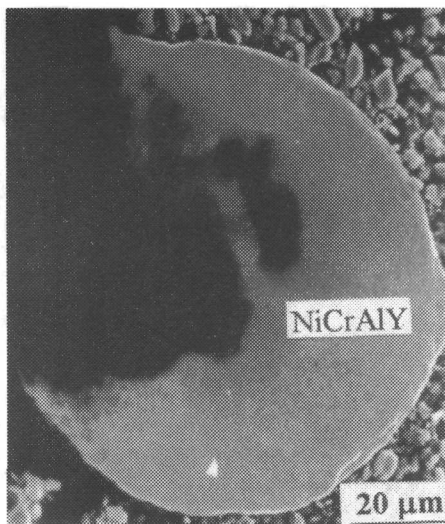


Fig. 5a. A bright field transmission electron micrograph showing the overall microstructure of the NiCrAlY powders.

Fig. 5b. A selected area diffraction pattern showing the  $\beta$ -NiAl and Ni<sub>5</sub>Y diffraction spots.

the most diverse solidification structure morphology. A typical powder structure is shown in Fig. 2. The EDX analysis of the overall composition of powder particles

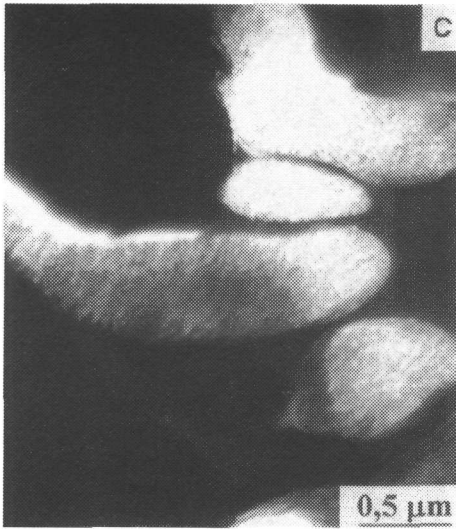


Fig. 5c. A dark-field image formed using a  $\beta$ -NiAl reflection.



Fig. 5d. A dark-field image formed using a  $\text{Ni}_5\text{Y}$  reflection.

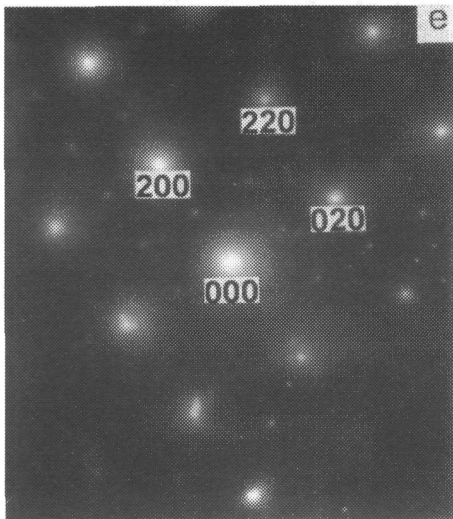


Fig. 5e. A selected area diffraction pattern showing the  $\gamma/\gamma'$  diffraction spots.

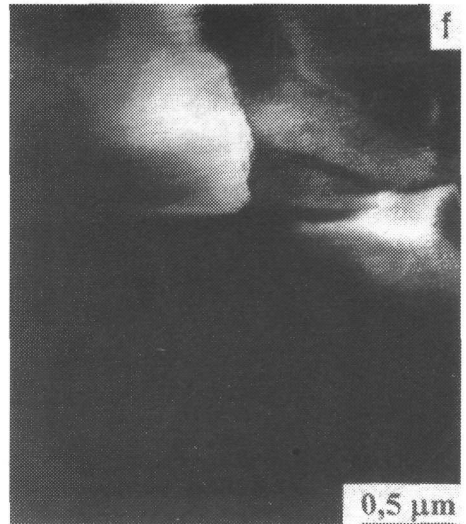


Fig. 5f. A dark-field image formed using a  $\gamma/\gamma'$  reflection.

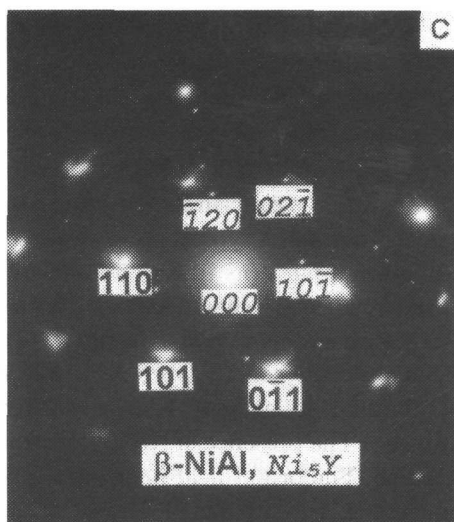


Fig. 6a. A bright field transmission electron micrograph showing the microstructure of the NiCrAlY powders.



Fig. 6b. A dark-field image formed using a  $Ni_5Y$  reflection.

Fig. 6c. A selected area diffraction pattern showing the  $\beta$ -NiAl and  $Ni_5Y$  diffraction spots.



resulted in a good agreement with the nominal composition. However EDX analysis of individual dendrites and grains revealed that they are of two types: Al rich





Fig. 7a. A bright field transmission electron micrograph showing the martensitic and  $\gamma/\gamma'$  phases in the structure of NiCrAlY powders.

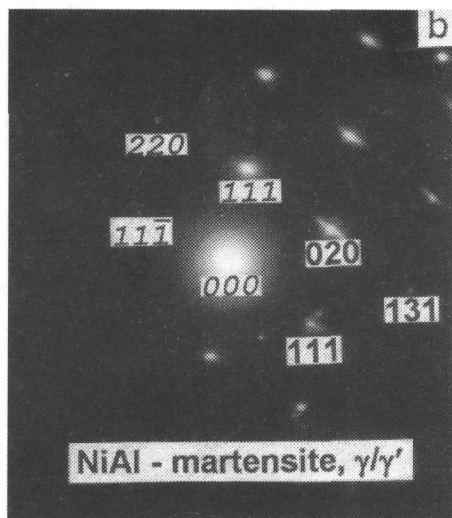


Fig. 7b. A selected area diffraction pattern showing the NiAl-martensite and  $\gamma/\gamma'$  diffraction spots.

dendrites with Al content in the range from 18 to 30 at.% and Al lean dendrites with Al content in the range from 5 to 13 at.%. As it can be seen in Fig. 3, they are of quite similar morphology. Y was found exclusively in the grain boundary regions at concentrations up to 7 at.%.

TEM observations of the thin foil sample shown in Fig. 4 revealed the fine grained microstructure with grain sizes rarely exceeding  $10\ \mu\text{m}$ . The powder microstructure of a typical appearance is shown in Fig. 5a. A selected area of electron diffraction patterns in Fig. 5b and 5e and the dark field images formed by appropriate reflexions shown in Fig. 5c and 5f revealed  $\beta$ -NiAl grains with  $B_2$  crystal structure and  $\gamma/\gamma'$  grains in the structure of the powders. Ni<sub>3</sub>Al ( $\gamma'$ ) was observed as a very fine coherent precipitate in the Ni base solid solution ( $\gamma$ ) matrix grains. Individual grains were often separated by intermetallic yttride Ni<sub>5</sub>Y as shown in Fig. 5d. The presence of Ni<sub>5</sub>Y yttride in the powder structure is confirmed in Fig. 6, as well. The bright field image in Fig. 7a reveals a martensitic phase in the powder microstructure. It was identified by electron diffraction as a martensitic NiAl phase with a tetragonal  $L1_0$  structure. The presence of the  $\gamma$  phase in the structure is confirmed in Fig. 8. SAED pattern in Fig. 8b refers to the lower right-side corner grain in Fig. 8a. The lower left-side corner grain is most probably a martensitic NiAl phase.



Fig. 8a. A bright field transmission electron micrograph showing the NiAl-martensite and  $\gamma$  phases in the structure of NiCrAlY powders.

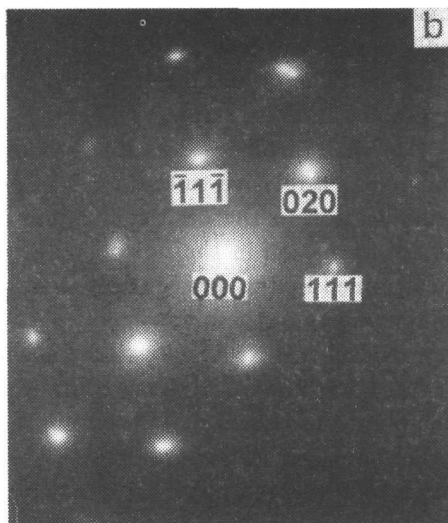


Fig. 8b. A selected area diffraction pattern showing the  $\gamma$  diffraction spots.

#### 4. Discussion of results

Light microscopy observations revealed an inhomogeneous solidification structure of NiCrAlY powders. EDX analysis showed that Al rich and Al lean grains can be found in the microstructure. Taking into account the results of the TEM observations as well as the published results [1, 2], the Al rich grains belong to the  $\beta$ -NiAl phase whereas the Al lean grains belong to the  $\gamma$  phase. Very little and very fine  $\gamma'$  precipitates were observed in the structure and so we consider the  $\gamma/\gamma'$  to belong to the group of Al lean grains. Yttrium was analysed by EDX in concentrations up to 7 at.%. This value is lower than expected in the Ni<sub>5</sub>Y yttride determined by electron diffraction. However, the yttrides in the NiCrAlY powders as shown in the TEM micrographs are so fine that they cannot be analysed with sufficient accuracy by EDX.

Both  $\beta$ -NiAl and martensitic NiAl give patterns with a diffuse intensity distribution. Hirabayashi et al. [3] showed that the diffuse intensity distribution in an electron diffraction pattern has an origin in a large elastic strain due to the large elastic anisotropy. Enami et al. [4] reported that diffuse streaks in  $\beta$ -NiAl patterns have to do with a lattice instability associated with martensitic transformation. Moreover, Chandrasekaran et al. [5] showed that highly defected



martensitic NiAl gives diffraction patterns of varying appearance depending not only on the fineness of the twins but also whether or not they are regularly distributed. The diffuse intensity patterns shown in Fig. 5b, 6c and 7b can also be explained in these terms.

AMDRY 962 powders with a nominal composition Ni<sub>22</sub>Cr<sub>10</sub>Al<sub>1</sub>Y can be considered as a relative to the  $\beta$ - $\gamma$  Ni-Cr-Al eutectic family of alloys. However, rapid solidification in the gas atomization process suppresses the diffusion and so the phase formation in the powders is closely related to the local chemistry which is determined by the degree of segregation. This is why it was possible to identify so many phases in the microstructure of powders.

Nickel rich Ni-Al alloys are known to transform martensitically [6–8]. Experiments have shown that alloys containing more than 63 at.% Ni when quenched from temperatures below 1000 °C contain the equilibrium phases NiAl and Ni<sub>3</sub>Al. On the other hand, when these alloys are quenched from temperatures above 1000 °C and examined microscopically a typically martensitic decomposition product appears in the microstructure. NiAl martensite was determined also in Ni-Cr-Al alloys [2, 9], what is in a good agreement with our results.

Anyhow, the presence of Y in the form of Ni<sub>5</sub>Y and the occurrence of NiAl martensite in the structure of powders implies some questions to be answered later on. As already mentioned, NiCrAlY powders are aimed for protective plasma sprayed coatings in hot corrosive or oxidizing environments at high temperatures. Yttrium is added to the alloy with the aim to improve the adherence of alumina or chromia scales. However yttrium bound in the Ni<sub>5</sub>Y yttride dissolves at temperatures higher than 1000 °C and as reported [1], it is entirely effective at temperatures above 1100 °C. On the other hand, this temperature range might be dangerous for NiCrAlY coatings because the martensitic transformation is commonly accompanied by volume changes. As NiCrAlY coating and alumina scales are in an intimate contact a volume change resulting from the phase transformation may have a detrimental effect on the spalling of Al<sub>2</sub>O<sub>3</sub> during cooling to ambient temperatures.

## 5. Conclusions

A procedure suitable for thin foil preparation of metal powders was shown and the microstructure of the NiCrAlY (AMDRY 962) powders was studied in this paper. The powder structure was found to consist predominantly of  $\beta$ -NiAl and  $\gamma$  grains. NiAl-martensite and  $\gamma/\gamma'$  phases were also determined in the structure. Yttrium was found in the Ni<sub>5</sub>Y yttride localized in the grain boundary regions.

## REFERENCES

- [1] SACRÉ, S.—WIENSTROTH, U.—FELLER, G.—THOMAS, L. K.: *Journal of Mat. Sci.*, 28, 1993, p. 1843.

- [2] KUPČENKO, G. V.—NESTEROVIČ, L. N.: *Struktura i svojstva evtektičeskich kompozicionnyh materialov*. Minsk, Nauka i tehnika 1986.
- [3] HIRABAYASHI, M.—WEISSMAN, S.: *Acta Met.*, 10, 1962, p. 25.
- [4] ENAMI, K.—HASUNUMA, J.—NAGASAWA, A.—NENNO, S.: *Scripta Met.*, 10, 1976, p. 879.
- [5] CHANDRASEKARAN, M.—BEYER, J.—DELAEY, L.: *Scripta Met.*, 27, 1992, p. 1841.
- [6] ROSEN, S.—GOEBEL, J. A.: *Trans. TMS – AIME*, 242, 1968, p. 722.
- [7] AU, Y. K.—WAYMYN, C. M.: *Scripta Met.*, 6, 1972, p. 1209.
- [8] SMIALEK, J. S.—HEHEMAN, R. F.: *Metall. Trans.*, 4, 1973, p. 1591.
- [9] HUANG, S. C.—HALL, E. L.—CHANG, M.—LAFORCE, R. P.: *Metall. Trans. A*, 17A, 1986, p. 1685.

Rukopis dodaný: 28.6.1996  
Rukopis upravený: 31.7.1996